

Bonding Characteristics of Cold Sprayed Copper Coating on Alumina Coated Q235 Steel Substrate

Guosheng HUANG*, Li MA, Lukuo XING, Xiangbo LI

State Key Laboratory for Marine Corrosion and Protection, Luoyang Ship Material Research Institute, 266237, Wenhai Road, Qingdao, Shandong Province, China

crossref <http://dx.doi.org/10.5755/j02.ms.25326>

Received 19 February 2020; accepted 29 May 2020

Cold spraying metallic coatings on ceramics (Ceramics Metallization) are widely concerned in electrical industry due to its high density, low oxidation and high electrical conductivity. However, the bonding reliability of the cold spraying coating on ceramics is usually considered to be poor since the metal particles don't experience melting. In the present work, the bonding quality of a cold spraying copper coating on a thermal sprayed alumina layer was examined. A pure copper coating was successfully deposited on Al₂O₃ coated Q235 steel substrate by cold spraying at 260 °C and 1.6 MPa using a pure copper powder. The bonding characteristics were studied by analyzing the surface, the cross-sectional microstructure of the coating and its interface after pull-off test. The results indicate that the high bonding quality (ranging from 8.26 MPa to 11.35 MPa) between copper coating and Al₂O₃ layer attributes to both metallurgical and interlock effect, which is mainly influenced by the hardness of the copper powders instead of Al₂O₃ surface roughness. The soft character of the pure copper powder makes it ready for deformation, subsequently interlocks with Al₂O₃, fills into the pores more completely, which increases the bonding quality between the copper coating and the Al₂O₃ layer.

Keywords: cold spray, thermal spray, ceramics, copper, bonding strength.

1. INTRODUCTION

Many research works indicate that it is hard to deposit thick metal coatings on ceramic substrate by cold spray (CS) method [1, 2]. To improve the bonding performance of metal coating on ceramics, the coating system needs to be carefully designed from raw powders, substrate types to spray parameters [3–5]. The reason is clear that a metal particle cannot easily adhere to ceramics substrate below its melting temperature. By referring to cold spray, it means a gas dynamic spray system developed by Papyrin [6], which comprises an air source that is connected by a gas passage to a heating unit, and in turn fed into a supersonic nozzle, a metal or metal mixed powder is accelerated to supersonic velocity and impacts onto a substrate, the substrate can be metal, ceramics, glass, polymer, wood and even paper [7]. It is believed that the coating is formed below the melting point of metal by large plastic deformation, the bonding mechanism is mainly mechanical interlock accompanied by local melting phenomenon [4]. Due to its low processing temperature, cold spray coating possesses number of advantages, such as high density, low oxidation and free of phase transition, and arouses numerous interests in many industries. Especially in the electronics industry and biomedical industry, cold spray method has been widely studied to coat aluminum and copper metal coatings on ceramics such as Al₂O₃, AlN, ZrO₂ and etc. [8–11]. It is easy to understand the bonding mechanism of ceramics on metals in cold spraying, most researchers consider that the ceramics particles embed into the metal and cannot form thickness pure ceramics layer. But it is much more

complicated for metallic coatings deposited on ceramics substrates, the bonding mechanism cannot be solely attributed to mechanical clamping, since strong bonds can be observed in many conditions such as Ti coatings deposited on Al₂O₃, copper on Al₂O₃, and aluminum coatings on AlN substrates [12, 13]. It was documented that the roughness of substrate, the pores size of substrate, the temperature of the substrate, and the thermal expansion ratio difference between metal and ceramics can affect the bonding type between metal and ceramics [12–14]. The first two factors result in metallurgical bonding between metal and ceramics, which improve the bonding quality. Increased substrate temperature has been found to increase adhesion strength in metal/ceramics interfaces as it reportedly allows for a stronger chemical bond [10, 11, 13–15]. It was also found that the types of ceramics also influence the bonding quality. Also, the coefficient of thermal expansion mismatch was not found to directly influence bond strength. Rather, a higher thermal conductivity of the substrate was assumed to have a positive effect as the interface contact temperature is lower. With a lower contact temperature, negative effects induced by the coefficient of thermal expansion mismatch between the metal and ceramics and tensile residual stresses are reduced [16]. S. I. Imbriglio studied the effect of different ceramics substrate roughness on the bonding behavior of Ti particles [17] and found that high roughness leads to “mechanical lock” between particles and substrate, while low roughness leads to metallurgical bonding. Pores also has a significant influence on the bonding behavior, ceramics with large pore need higher force to pull off the deposited splat from the pore. On the other hand, single Ti splat deposited on zirconia only showed gaping near the center of the particle and bonding near the edge [18]. Although many types of metal/ceramics coating systems

* Corresponding author. Tel.: +86-532-68725121; fax: +86-532-68725001. E-mail address: huanggs@sunrui.net (G.S. Huang)

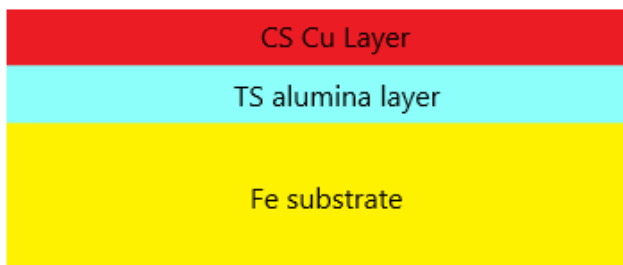
were deposited successfully by cold spray, some of the bonding mechanisms were also proposed by the researchers. However, systematic designing is needed to produce a new reliable metal/ceramic coating system by cold spray. Few works had been done to study the influence of particle hardness on the bonding behavior of metal coating on ceramics, which has significant influence on the bonding behavior of metal on ceramics.

In the present work, a copper coating was deposited by cold spraying on Al₂O₃ coated Q235 steel substrate, the mechanical properties and bonding characteristics were discussed by observing the microstructure and interface between metal coating and ceramics substrate to investigate the factors that influence the bonding qualities.

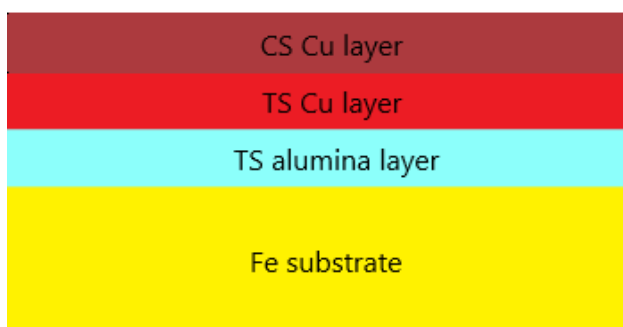
2. EXPERIMENTAL SET-UP AND INSTRUMENTATION

2.1. Structure of the Cu/Al₂O₃ coating

The structure of the Cu/Al₂O₃ coating system and the designing purpose were illustrated in Fig. 1 a. The Al₂O₃ layer serves as an insulation layer to separate copper coating from electrical connecting to steel substrate in case of galvanic corrosion, which can also guarantee the release rate of Cu(I) under the cathodic protection condition. In case of unable to deposit coating on ceramics directly and improving bonding strength of a cold spraying (CS) coating on Al₂O₃ ceramics, a thermal sprayed (TS) copper bond layer was also deposited by flame spraying on ceramics before cold spraying copper coating for comparison purpose, which had the structure as shown in Fig. 1 b.



a

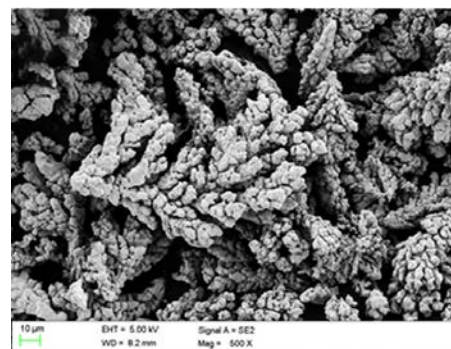


b

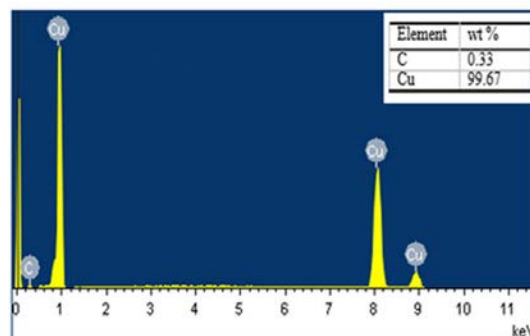
Fig. 1. Structure of copper/Al₂O₃ composite coating system: a – cold sprayed (CS) copper coatings on thermal sprayed (TS) Al₂O₃ layer; b – CS copper coatings on TS copper/Al₂O₃ layer

2.2. Raw powders

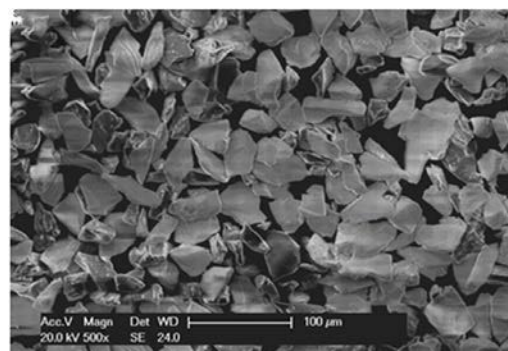
A commercial pure copper powder was used to deposit both cold spray coating and thermal spray coating, which was provided by Hebei Zhuhang Powder Company (Shijiazhuang, China). The morphologies of the powders were observed using an SEM (XL-30 Scanning Electron Microscope, manufactured by Philips, Netherlands). The melting crushed Al₂O₃ powder was a pure powder as shown in Fig. 2 c also from Hebei Zhuhang Powder Company for coating Al₂O₃ layer. The nominal hardness of the copper powder was about 45-55 HV_{0.2} (data got from manufacturer). It was worth noting that the hardness of this kind of copper particle was much lower than that of most other kinds of copper particles with hardness ranging from 120-150 HV_{0.2}.



a



b



c

Fig. 2. Characteristics of electrolysis pure copper powders: a – SEM morphology of electrolysis copper powders used for cold spraying; b – EDS spectrum of electrolysis copper powders; c – SEM image of melting and crashing alumina powders used for Al₂O₃ coating

Another hard copper powder was used to exam the influence of powder hardness effect on the bonding quality. The hardness of the copper powders was tested with a hardnessmeter (HXD-1000 digital hardness tester, manufactured by Shanghai Tai Ming, China). The details about the hardness test: Firstly, the raw powders were mixed with epoxy resin with a content about 80 % (vol.), filled into a PE tube, then solidified at 80 °C in an oven. The surface was polished to 600# with sandpaper and measured with the hardnessmeter.

2.3. Cold spraying coating

The base metal was Q235 steel, sandblasted for 15 min to get a roughness above 65 μm (R_z). The substrate was preheated to about 90°C to avoid the effect of moisture before flame spraying. An oxygen acetylene flame spray system (SHF-E2000, Shanghai Liangshi Company, China) was adopted for coating Al₂O₃ insulating layer. The melting crushed Al₂O₃ powder was a pure powder as shown in Fig. 2 c from Hebei Zhuhang Powder Company. The oxygen pressure was 0.6 MPa; acetylene pressure was 0.1 MPa, and the volume ratio of oxygen to acetylene was 1:1.2 for the preheating gas. The surface roughness was controlled by varying the spraying pressure and measured by a probe roughness meter (elcometer-GRIT/SHOT). It was found that the roughness of the coating surface increased as the pressure decreased. The copper bond layer was also sprayed with the same spraying parameters as mentioned above.

As-sprayed Al₂O₃ coating and Cu/ Al₂O₃ coating were used as substrates. A self-made cold spray system (State Key Laboratory for Marine Corrosion and Protection, Qingdao, China) was used to deposit the copper coatings, which has a key structure characteristic described in Table 1. The gas parameters adopted in this study are as follows: the pressure in prechamber was 1.6 MPa, the temperature in prechamber was 558 K ± 20 K, the powder feeding rate was about 1.5 g/s, the transverse speed of nozzle was 20 mm/s and the distance between the nozzle to the substrate was 25 mm. All samples were prepared using the same parameter. It worth noting that the inner shape of the nozzle is a transition from circle at the throat to rectangular at the exit.

Table 1. Nozzle structure summary and spraying parameters in present work used for CS-6000 cold spray system

Parameters	Value
Expansion ratio	6.36
Diameter of nozzle throat	2.00 mm
Length of converging part	10 mm
Length of diverging part	100 mm
Dimension of exit	2 mm × 10 mm
Standoff distant from nozzle exit to substrate	25 mm
Pressure in prechamber	1.6 MPa
Temperature in prechamber	558 ± 20 K
powder feeding rate	1.50 g/s
Spraying angle	90° ± 5°
Transverse speed of nozzle	25 mm/s

2.4. Microstructure observations

The samples for Scanning Electron Microscope (SEM) observation were cut through the cross-section with size of

10 mm × 10 mm, abraded with emery paper to 2000 number, washed with acetone and distil water. The as sprayed coating surface of the CS copper coating, the TS alumina coating and the TS copper/alumina coating were observed with SEM, as well as the alumina layer and some scattered copper particles at the boundary area.

The pull-off bonding strength test was carried out on a stretcher (DWD-20 computer controlled tester, manufactured by Shanghai, China) according to the Pull-off Strength Test Method standard. The specimen for bonding measurement were disks with diameter 25 mm and thickness 3 mm. The test specimen was bonded to the fixture by an E-7 Glue, the stretching rate was 0.03 mm/s in constant. The maximum force (F , N) as the coating broke from the substrate was recorded to calculate the bonding strength. Then the bonding strength can be calculated by Eq. 1. Both side of the broken surface was observed under SEM including alumina side and copper coating side.

$$BS = F/A, \quad (1)$$

where BS is the bonding strength of samples, A is the area of disks.

3. RESULTS

3.1. Characteristics of raw powders

The morphologies of the powders are shown in Fig. 2. The copper particles have the diameter distribution from 10 μm to 45 μm with a wheatear shape, which is a typical shape of electrolytic copper powder as shown in Fig. 2 a. The EDS spectrum indicates that the powder is nearly oxygen free as shown in Fig. 2 b. The melting crushed Al₂O₃ powder is a pure powder as shown in Fig. 2 c. It is worth noting that the hardness of this kind of copper particle is much lower than that of most other kinds of copper particles with hardness ranging from 120–150 HV_{0.2}. It can be seen that the hardness of the soft copper powder is only 29.0 ± 1.7 HV_{0.2} listed in Table 2. And the hard copper powder has a hardness of 119.8 ± 3.7 HV_{0.2}.

Table 2. Hardness of the copper particles used for investigating the influence of powder hardness on bonding quality

Particle number	Soft powders (HV ₀₂)	Hard powders (HV ₀₂)
1	28.6	117.8
2	31.5	119.8
3	26.7	115.5
4	28.9	121.7
5	29.2	124.2
Average	29.0 ± 1.7	119.8 ± 3.7

The Vickers microhardness variation of copper coating with the distance from interface to surface prepared by cold spraying (b) are listed in Table 3. It can be seen that the microhardness has the highest value at the interface and the lowest value at the surface both for cold sprayed copper coating on TS Copper/Al₂O₃/steel and Al₂O₃/steel. The cold sprayed copper coating on Al₂O₃/steel is a little harder than that of the cold sprayed copper coating on TS Copper/Al₂O₃/steel. For the cold spray coating, the microhardness of the coating increases from surface

(32.1 HV) to interface (38.5 HV). The reason is that the subsequent particles have a certain impact and strengthening effect on the previously sprayed coating during the spraying process, so the hardness of the coating near the interface is usually harder than that of the coating near the surface. However, the hardness of the coating is influenced by the substrate, it means that the hardness of the coating near the interface is a comprehensive value of coating and substrate. The situation of cold sprayed copper coating on TS Copper/Al₂O₃/steel is the same to cold sprayed copper coating on Al₂O₃/steel. It is worth noting that no good quality coating was obtained with the harder copper coating.

Table 3. Hardness variation through the thickness direction of cold sprayed copper coatings on Al₂O₃/ steel and cold sprayed copper coatings on TS Copper/Al₂O₃/steel

Depth from interface to surface (approximate value)	Hardness (HV _{0.2})	
	Cold sprayed copper coatings on Al ₂ O ₃ /steel	Cold sprayed copper coatings on TS copper/Al ₂ O ₃ /steel
Interface	–	–
100	38.5	34.4
200	37.5	33.7
300	34.6	33.9
400	33.2	32.6
500	32.1	–
Surface	–	–

3.2. Characteristics of CS Copper/Al₂O₃ coating on Q235 steel

The macro morphologies of the TS alumina coating on steel and CS copper coatings on the alumina coated steel are shown in Fig. 3. It can be seen from Fig. 3 a that the ceramic coating has a relative even surface. Roughness test indicates that the average surface roughness is $1.25 \pm 0.05 \mu\text{m}$ (R_z) in its as-sprayed status. The surface roughness of the TS copper coating is about $12.5 \pm 0.1 \mu\text{m}$ (R_z). The roughness of the samples and the bonding strengths are listed in Table 4. The as-sprayed coatings both have a full dense appearance under the magnification of 200 times. The total thickness for both of the cold sprayed coating is about 0.6 mm, and each pass can build up about 0.15 mm thickness coating (four passes in coating process). It can be seen from Fig. 3 c–Fig. 4 d that the

coatings both have uneven surface morphology at the overlap location, which is because the fluctuating of spraying parameters of the cold spray system and the velocity difference between particles at different location of the nozzle exit along the length direction (10 mm). The photo of spraying process is shown in Fig. 3 b, it can be seen that the copper coatings were deposited much easily both on CS copper layer and TS alumina layer. Both of the coatings have the similar thickness of 500–600 μm , thus the deposition efficiencies are also the similar to each other. The color of the CS copper coating is fresh red, which is different from the TS copper coating dark red. Four passes of spraying build a coating with the total thickness more than 500 μm , which is a bit different from some previous research that thick coating will lead to coating abscission from ceramics substrate because of the expansion ratio difference.

Table 4. Roughness of flame sprayed Al₂O₃ coating on Q235 steel

Sample	Roughness R_z , μm	BS, MPa
As-received Al ₂ O ₃ coating on Fe	3.2 ± 0.1	8.26, 10.17, 11.35
As-received Al ₂ O ₃ coating on Fe	1.2 ± 0.1	9.92, 9.37, 9.16
2000# diamond grinding Al ₂ O ₃ coating on Fe	0.7 ± 0.1	6.66, 10.42, 7.17
As-received copper coating on Al ₂ O ₃ /Fe	12.5 ± 0.1	12.22, 14.13, 11.52

The micro morphologies of the CS Copper coatings on alumina/steel are shown in Fig. 4. It can be seen from Fig. 4 a that the ceramic coating has a relative even surface under low magnification of $\times 50$. The surface morphology is a typical thermal sprayed coating with splashed melting particles on surface as shown in Fig. 4 b. There are some pores, which can be found under high magnification of $\times 50$ as arrow pointed. The diameter of the pores ranges from about several microns to ten microns, but there is no any crack that can be found on the surface of the alumina layer. There are many small splashed alumina particles on the surface, which may have low bonding quality and influence the deposition of subsequent cold sprayed copper coating.

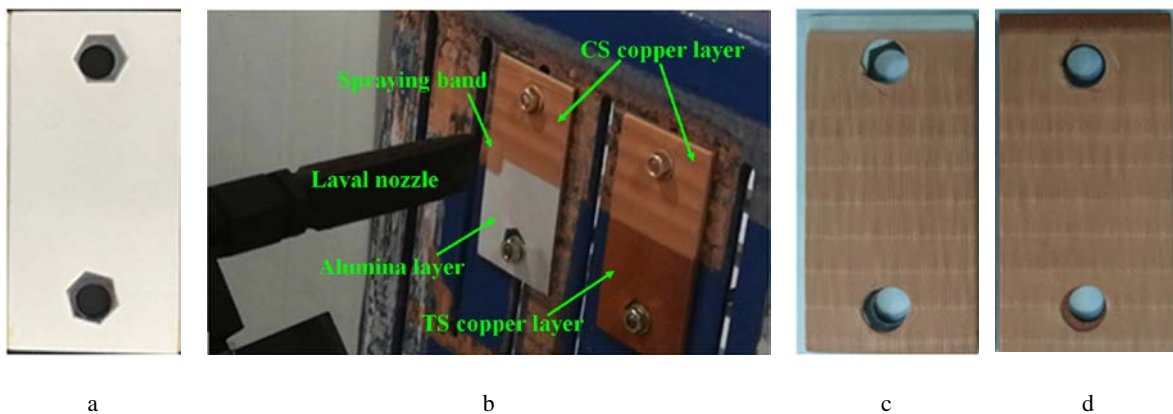


Fig. 3. Macro morphology of specimens used for test: a – thermal sprayed Al₂O₃ coatings on steel; b – coating deposition process during cold spraying on alumina and TS copper layer; c – cold sprayed copper coatings on Al₂O₃/steel; d – cold sprayed copper coatings on TS copper/Al₂O₃/steel

At most location of the bulk coating area, the copper particles deform completely as shown in Fig. 4 c, the surface morphology of deformed particle is totally different from the powders in this area and bond to each other compactly. But some particles did not experience enough deformation as shown in Fig. 4 d as pointed out by arrows, the particles have the initial shape of the raw

powders. This could be the up side of the copper particles, the down side may be different from it, which could be found after the pull off test (below in Fig. 7). Although copper particles are soft and ready to deform, partially deformation occurs to some particles with low velocity with larger diameter.

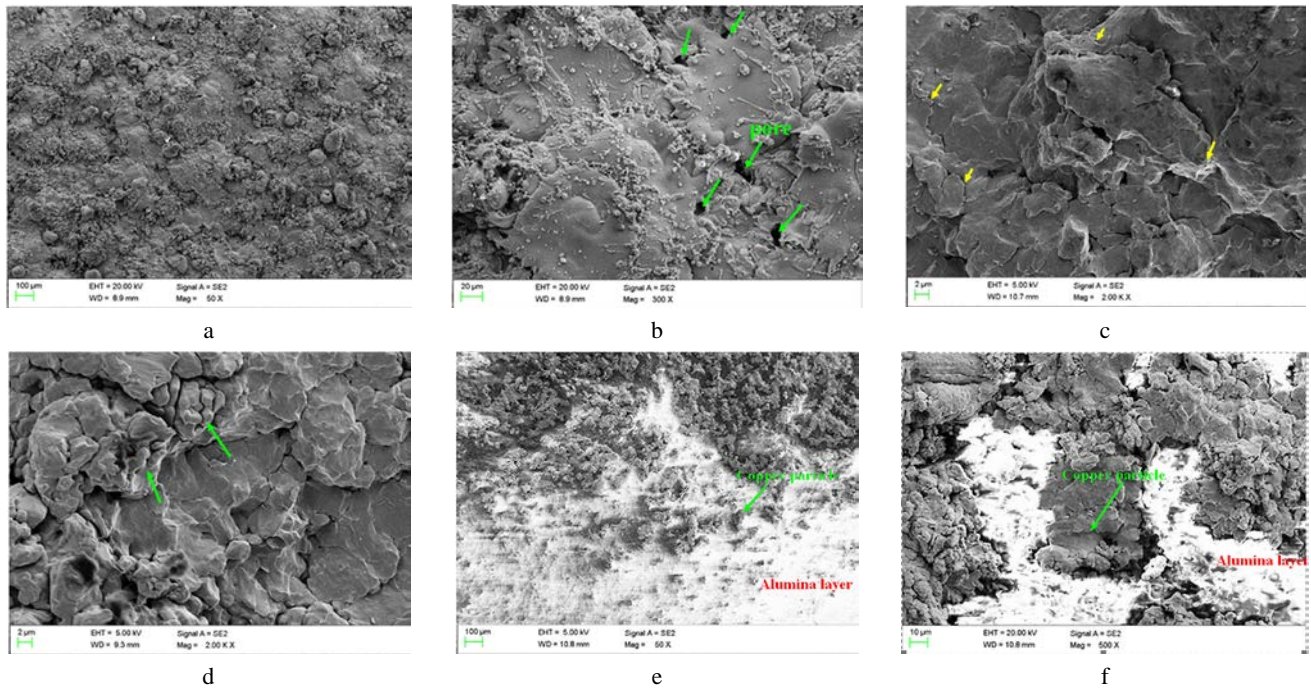


Fig. 4. Micro morphology of specimens used for test: a–thermal sprayed Al_2O_3 coatings on steel $\times 50$; b–thermal sprayed Al_2O_3 coatings on steel $\times 300$; c–cold sprayed copper coating on $\text{Al}_2\text{O}_3/\text{steel}$ $\times 2000$; d–cold sprayed copper coating on $\text{Al}_2\text{O}_3/\text{steel}$ $\times 2000$; e–boundary of cold sprayed copper coating and Al_2O_3 substrate; f– deposited single copper particle on $\text{Al}_2\text{O}_3/\text{steel}$

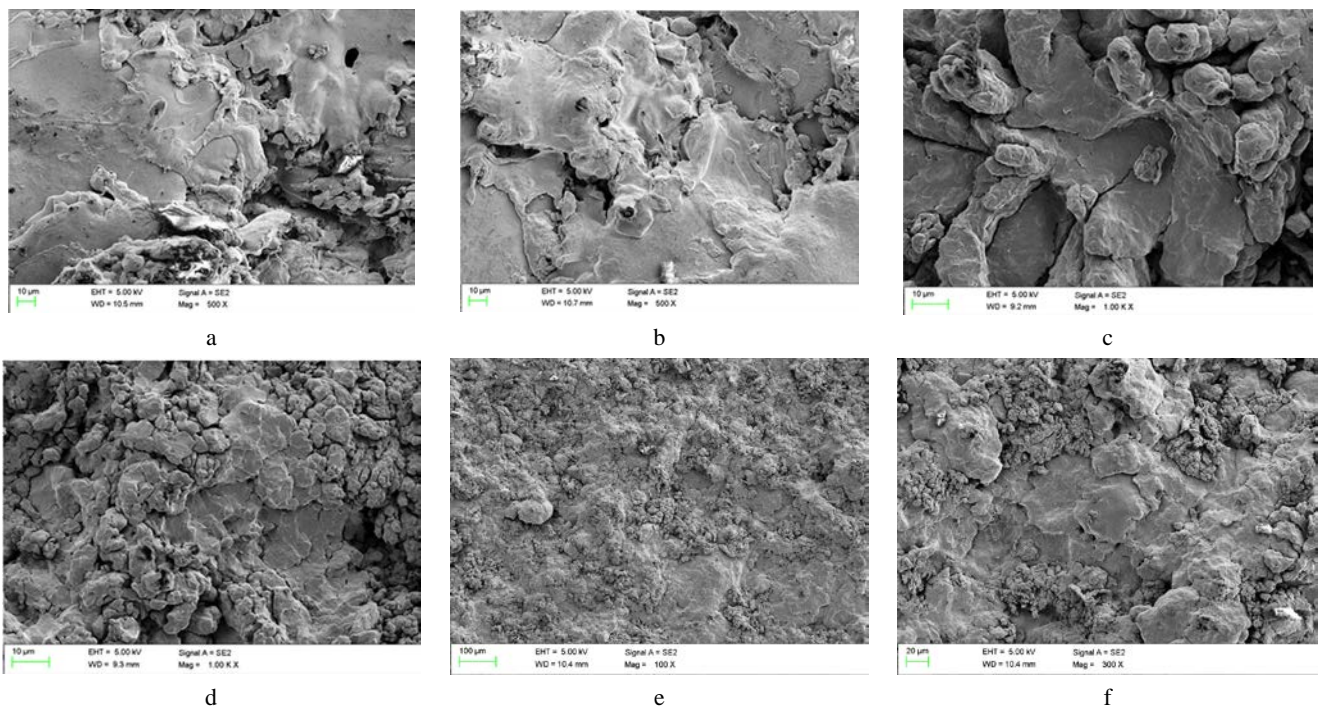


Fig. 5. Micro morphology of specimens used for test: a–thermal sprayed copper coatings on $\text{Al}_2\text{O}_3/\text{steel}$ $\times 500$; b–thermal sprayed copper coatings on $\text{Al}_2\text{O}_3/\text{steel}$ $\times 500$; c–cold sprayed copper coating on $\text{Cu}/\text{Al}_2\text{O}_3/\text{steel}$ $\times 1000$; d–cold sprayed copper coating on $\text{Cu}/\text{Al}_2\text{O}_3/\text{steel}$ $\times 1000$; e–boundary of cold sprayed copper coating and TS Cu; f–single copper particle deposited on $\text{Cu}/\text{Al}_2\text{O}_3/\text{steel}$

Deformation of the entire particle is impossible because the energy is rapidly absorbed by the deformation of particle and the crater of substrate if the particle has not enough energy (velocity). The scattered copper particles deposited at the edge of the coating show no defect and gap between the particles and the Al_2O_3 substrate as shown in Fig. 4 e–f. The white area with poor visual quality is low electrical conductivity alumina, the dark area is the deposited high electrical conductivity copper particles.

Fig. 5 shows the micro morphology of cold sprayed copper coating on the TS Cu/ Al_2O_3 /Steel. It can be seen from Fig. 5 a that the TS Cu/ Al_2O_3 /Steel has a relative even surface. The surface morphology is a typical thermal sprayed coating of splashed melting particles as shown in Fig. 5 b. There are some pores, which can be found under high magnification of $\times 500$. The deformation of CS copper particles as shown in Fig. 5 c–d is similar to that of copper particles on the Al_2O_3 /steel as shown in Fig. 4 c–d, but the deformation ratio is lower than the former. It can be seen that there are much more undeformed particles on the TS Cu coating. This could be the reason that the soft substrate exhaust part of the energy of high velocity copper particles, so the deformation is lower on TS copper layer. At the boundary of TS copper coating and CS copper coating, many scattered copper particles can be found as shown in Fig. 5 e–f. It is hard to identify the cold sprayed particles by color, but the shape of particle is completely different between cold sprayed particles and the TS copper coating. The cross-sectional SEM morphology of the CS Copper coatings on Al_2O_3 /steel is shown in Fig. 6. It can be seen that the coating has two layers in Fig. 6 a. One layer on the steel substrate is the Al_2O_3 layer, another layer is the copper layer on the Al_2O_3 layer. The thickness of the coating at different part is different. The copper layer ranges from $400\ \mu\text{m}$ to $600\ \mu\text{m}$. The copper coating contacts with the Al_2O_3 layer intimately. The Al_2O_3 layer has a roughness about $20\ \mu\text{m}$ from the profile of the cross-sectional surface, which is much coarser than as-received TS Al_2O_3 coating samples. Apparently, the impacting has a coarsen effect to the Al_2O_3 layer. But the reason is not clear, both the deformation and crack may lead to Coarsening effect for ceramics surface. The interface between CS copper layer and the TS copper layer could not be observed as shown in Fig. 6 b, which is due to the impaction of cold spray copper particles on TS copper layer. Similar to cold spray, the TS copper layer is densified by the impaction of cold spray copper particles, as in cold spray process the former deposited layer is densified by the latter impaction of the particles. And due to this difference for former and latter deposited layer, cold spray coating has a gradient structure, in which the interface has a high density and the surface has a low density.

3.3. Bonding characteristics of CS Copper coating on Al_2O_3 /steel

The bonding strength of six tested samples ranging from 8.26 to 11.35 MPa indicates that the bonding quality is rather good between the CS copper layer and the Al_2O_3 ceramics layer. The typical morphologies of the samples after pull-off-strength test are shown in Fig. 7. It can be

seen that all samples broke off from the interface between the Al_2O_3 layer and the CS copper layer, which indicates that the bonding strength of CS copper layer is lower than that between the interface of steel substrate and Al_2O_3 layer.

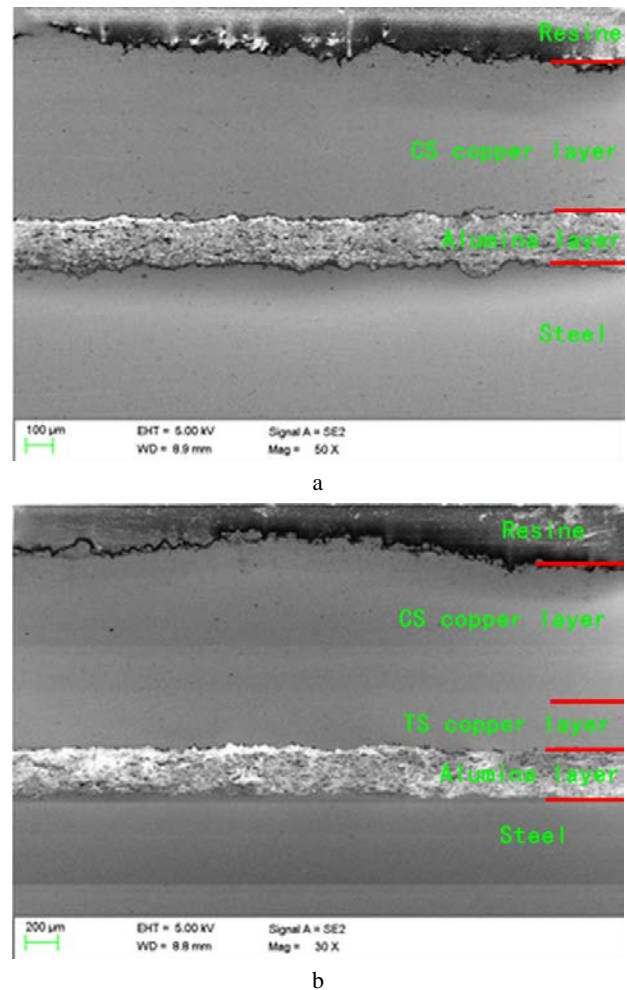


Fig. 6. Cross-sectional micro morphology of specimens: a–cold sprayed copper coating on thermal sprayed copper/ Al_2O_3 coated steel; b–cold sprayed copper coating on Al_2O_3 coated steel

Fig. 7 a shows macro morphology of the Al_2O_3 layer side and Fig. b shows the CS copper layer side. There are many copper residuals left on the Al_2O_3 layer side, and there are no Al_2O_3 particle left on the copper layer observed by naked eye. Former investigations revealed that it is possible to deposit well-adhering metallic coatings on atomically smooth ceramics. This led to the conclusion that mechanical interlocking is not always a necessary precondition for bonding. The jet phenomenon around the deformed particles (labeled in Fig. 4 and Fig. 7 with yellow arrows) indicate that local melting around the particles occurs for metal particles both at the interface and on the surface. A combination of recrystallization processes induced by adiabatic shear processes and heteroepitaxial growth might be an explanation for the observed high adhesion strengths [8]. To clarify the influence of the roughness of the Al_2O_3 on the bonding quality, different roughness Al_2O_3 coatings were controlled by changing the flame spraying parameters. Table 1 lists

the roughness of the Al_2O_3 layers and its corresponding bond strength. The bond strength of copper coating on Al_2O_3 layer varies little among the parallel samples, although the roughness of present work is much higher than that of the previous research [4]. It can be seen that cold spraying copper coating have good bonding quality on both coarse Al_2O_3 surface and smooth Al_2O_3 surface. The roughness has little effect on the bonding quality of cold spraying copper coating on Al_2O_3 ceramics. The fracture occurs at the interface between copper and Al_2O_3 for both of cold sprayed copper coating on Al_2O_3 and cold sprayed copper coating on TS copper/ Al_2O_3 . It can be found from Fig. 7 c–d that there is no crack existing at the bottom of the alumina layer. It can be seen from Fig. 7c–d that there

are also some alumina residuals (as pointed by arrows) left on the CS copper layer side, which is apparently contributed to the poor bonding quality of the alumina particles to alumina layer or eroded off by impaction of copper particles. The EDS as shown in Fig. 8 shows that alumina particles distribute randomly on the copper coating side, which means that the alumina particles were pulled off from the alumina coating surface. According to the diameter and the morphology of alumina substrate after pull-off tests, it is most probably that the splashed alumina particles were pulled off to the copper coating side. As to alumina layer side, the micro morphology indicates many copper residuals on it (as pointed out by arrows in Fig. 7 e–f.

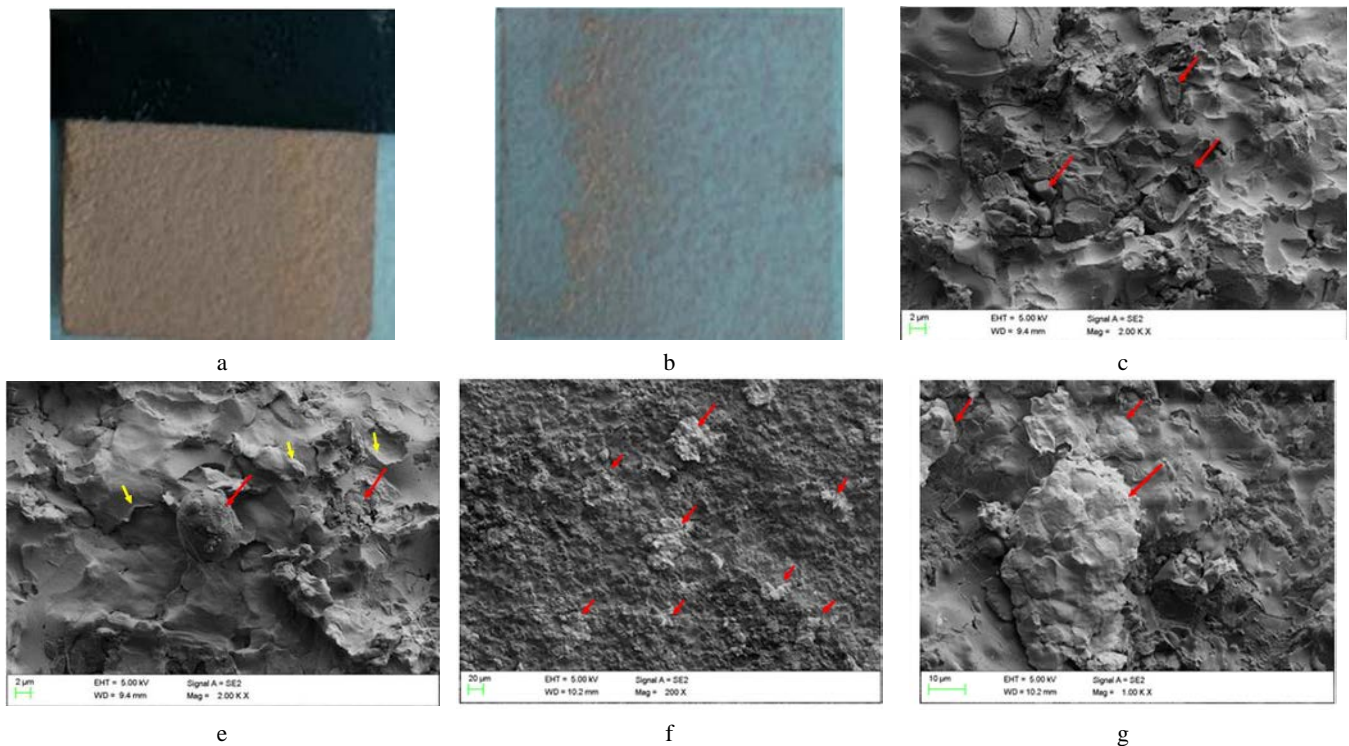


Fig. 7. Macro-morphologies and micro-morphologies of copper coating after pull-off strength test: a–macro morphology of cold sprayed copper coatings on $\text{Al}_2\text{O}_3/\text{steel}$: copper coating side; b–macro morphology of cold sprayed copper coatings on $\text{Al}_2\text{O}_3/\text{steel}$: $\text{Al}_2\text{O}_3/\text{steel}$ side; c–micro morphology of cold sprayed copper coatings on $\text{Al}_2\text{O}_3/\text{steel}$: copper coating side; d–micro morphology of cold sprayed copper coatings on $\text{Al}_2\text{O}_3/\text{steel}$: copper coating side; e–micro morphology of cold sprayed copper coatings on $\text{Al}_2\text{O}_3/\text{steel}$: $\text{Al}_2\text{O}_3/\text{steel}$ side; f–micro morphology of cold sprayed copper coatings on $\text{Al}_2\text{O}_3/\text{steel}$: $\text{Al}_2\text{O}_3/\text{steel}$ side

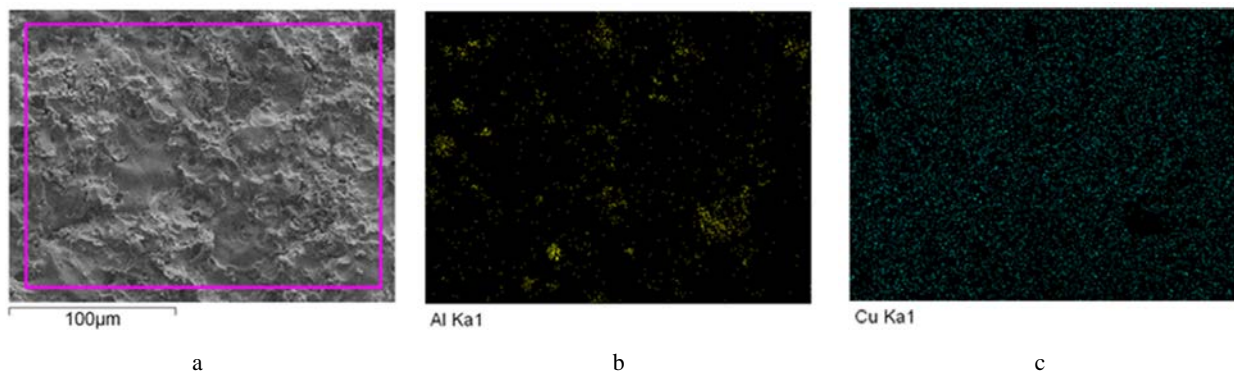


Fig. 8. SEM observation for copper coating side: a–micro-morphology of copper coating after pull off strength test; b–Al element distribution on the surface of the interface; c–Cu element distribution on the surface of the interface

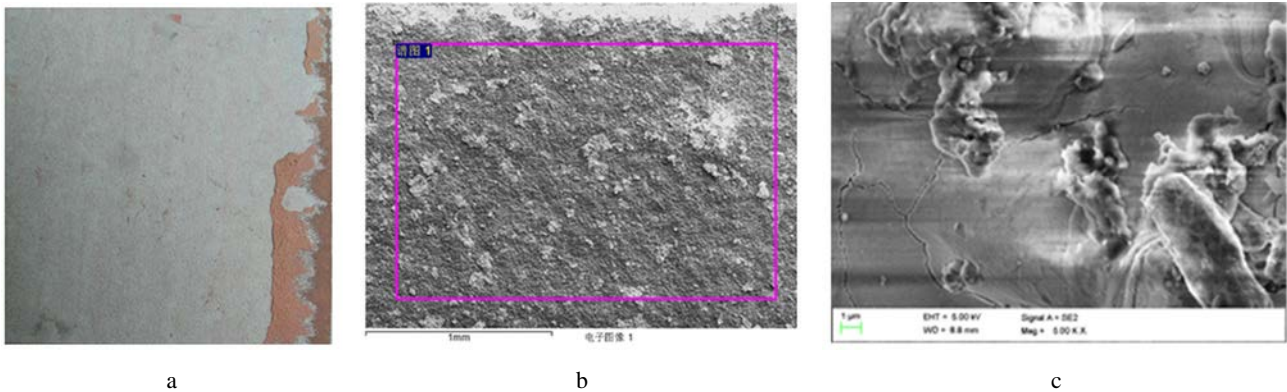


Fig. 9. a – macro-morphology of cold sprayed copper coating using harder copper particles; b – micro-morphology of copper residual on the surface of Al_2O_3 ; c – magnification morphology of Al_2O_3 after impacting (cracks induced)

The residuals have a very thin thickness, apparently, the bonding strength between alumina layer and the particle is higher than the yielding strength of the particle itself, then the thin copper residuals can be pull off from the particles and left on the alumina layer. Principally, the yielding strength of the particle is much high than bonding strength, but it dramatically decreases as it experiences high plastic deformation.

It is also an interesting phenomenon that there is no small splashed Al_2O_3 particle left on the Al_2O_3 surface, which can verify the pull-off of small Al_2O_3 particles. This phenomenon can decrease the bonding quality of the CS copper layer, thus the bonding quality will be promoted if sintered alumina substrate is used. It is no need to worry about the potential crack of alumina induced by high velocity copper particles impacting since the pure copper has a very soft character. Besides the soft character, copper is believed to be an almost ideal material for cold spraying, which is ready to deform since it has a very low resistance to strain [5]. Based on above experimental results and analysis, it is believed that surface roughness has little influence on the bonding quality of the copper coating since soft powders were used. The reason can be proposed as follows: roughness is not the key factor that determines the deposition of copper coating in present coating system, the more important parameter is the hardness of the copper powders. It can be seen from Fig. 8 that the deposition of a harder copper powder is totally different from the soft one at the same spraying parameter. There are still many copper particles left on the alumina layer side, but the coating has a very poor bonding quality even no complete coating formed. More cracks can be found on the alumina layer than soft copper powder as shown in Fig. 7 f. It is mostly because the harder copper particle deforms less and more energy was transferred to the alumina layer and led to cracks. Consequently, the occurrence possibility of local melting, interlocking to roughness substrate and embedding to pores decreases. It is worth noting that it is hard to get the exact relationship between the bonding quality and the hardness of powder, which is mainly because that no suitable method to measure the accurate hardness of the wheater shape powder. As a result, the bonding strength decreases. The bonding behavior of a metal particle on ceramics is different from that on metal substrate. It is believed that the coating has the highest bonding quality when the particle and the substrate has the

same hardness [19]. Under this situation, the particle experiences similar deformation with the substrate, and this kind of impaction leads to perfect contacting. But for ceramics substrate, the deformation mostly occurs to metal particle, the substrate is considered to be rigid and will not be impacted to form remarkable crater. Theoretically, the bonding strength on ceramics could be improved by increasing the surface roughness. But many previous researches indicate that metallurgical bonding occurs at the interface between metal and ceramics [12–14]. Previous experiments indicate that metal particles will not adhere to low roughness metal surface or has poor bonding strength with metal. While for ceramics substrate, crack and detachment of coating and substrate frequently happens at the present spraying parameter with other powder such as aluminum and titanium. That is the situation like Fig. 9 in present research.

4. CONCLUSIONS

The present work demonstrates successfully deposited a thick copper coating on an Al_2O_3 coated Q235 steel substrate by cold spray at 260 °C and 1.6 MPa using pure copper powders, compared the different surface roughness and powder hardness on the deposition behavior of copper particles, investigated the microstructure properties of cold sprayed copper coating on Al_2O_3 coated steel. Based on the experimental results, the following conclusions can be drawn. The CS copper coating on $\text{Al}_2\text{O}_3/\text{Fe}$ substrate has relatively good physical properties, the adhesion strength ranges from 8.26 to 11.35 MPa. Surface roughness has little effect on the bonding quality of cold sprayed copper coating on Al_2O_3 coated steel. The raw particle hardness is the main determined effect that influences the bonding quality because a soft particle can experience much larger deformation on ceramics substrate. The finding of present work provides a reliable ceramic metallization way by softening the particle hardness or selecting softer materials instead of by elevating the particle velocity to get high bonding strength, which is harmful to the interface bonding quality because crack crush may be induced on ceramics by high velocity impactations of metal particles.

Acknowledgments

The project was supported by The State Key Laboratory for Marine Corrosion and Protection, Luoyang Ship Material Research Institute (Grant No. JS1802).

REFERENCES

1. **Ding, R., Li, X.B., Wang, J., Xu, L. K.** Electrochemical Corrosion and Mathematical Model of Cold Spray Cu-Cu₂O Coating in NaCl Solution-Part I: Tafel Polarization Region Model *International Journal of Electrochemical Science* 8 (1) 2013. pp. 5902–5924. <https://doi.org/10.1166/sl.2013.2512>
2. **Huang, G. S., Xing, L.K., Li, X.B., Wang, H.R.** Antifouling Behaviour of a Low-Pressure Cold-Sprayed Cu/Al₂O₃ Composite Coating *International Journal of Electrochemical Science* 11 (1) 2016: pp. 8738–8748. <https://doi.org/10.20964/2016.10.02>
3. **Ichikawa, Y., Tokoro, R., Ogawa, K.** Micro-Scale Strength Evaluation for Bonding Interface of Cold Sprayed Coatings *Materials Science Forum* 879(P.T.1) 2016: pp. 795–800. <https://doi.org/10.4028/www.scientific.net/MSF.879.795>
4. **Dagmar, D., Bernhard, W., Thomas, L., Thomas, G., Sabine, K.** Evolution of Microstructure of Cold-Spray Aluminum Coatings on Al₂O₃ Substrate *Advanced Engineering Materials* 14 (4) 2011: pp. 275–278. <https://doi.org/0.1002/adem.201100261>
5. **Drehmann, R., Grund, T., Lampke, T., Wielage, B., Manyoats, K., Schucknecht, T., Rafaja, D.** Splat Formation and Adhesion Mechanisms of Cold Gas-Sprayed Al Coatings on Al₂O₃ Substrates *Journal of Thermal Spray Technology* 23 (1–2) 2014: pp. 68–75. <https://doi.org/10.1007/s11666-013-9966-z>
6. **Papyrin, A.** Cold Spray Technology *Advanced Materials and Processes* 159 (9) 2001: pp. 49–51. <https://doi.org/10.1002/1527>
7. **Assadi, H., Gärtner, F., Stoltenhoff, T., Kreye, H.** Bonding Mechanism in Cold Gas Spraying *Acta Materialia* 51 (15) 2003: pp. 1079–1088. [https://doi.org/10.1016/S1359-6454\(03\)00274-X](https://doi.org/10.1016/S1359-6454(03)00274-X)
8. **Drehmann, R., Grund, T., Lampke, T., Wielage, B., Manyoats, K., Schucknecht, T., Rafaja, D.** Interface Characterization and Bonding Mechanisms of Cold Gas-Sprayed Al Coatings on Ceramic Substrates *Journal of Thermal Spray Technology* 24 (1–2) 2015: pp. 92–99. <https://doi.org/10.1007/s11666-014-0189-8>
9. **Kashirin, A.I., Klyuev, O.F., Buzdygar, T.V.** Apparatus for Gas-Dynamic Coating, US Patent 6402050 B1, 2002.
10. **Maev, R.G., Leshchynsky, V.** Introduction to Low Pressure Gas Dynamic Spray: Physics & Technology, Wiley-VCH. 2, 2008: pp. 85–99. <https://doi.org/10.1002/9783527621903.ch2>
11. **Donner, K.R., Gaertner, F., Klassen, T.** Metallization of Thin Al₂O₃ Layers in Power Electronics Using Cold Gas Spraying *Journal of Thermal Spray Technology* 20 (1–2) 2011: pp. 299–306. <https://doi.org/10.1007/s11666-010-9573-1>
12. **Ernst, K.R., Braeutigam, J., Gaertner, F., Klassen, T.** Effect of Substrate Temperature on Cold-Gas-Sprayed Coatings on Ceramic Substrates *Journal of Thermal Spray Technology* 22 (2–3) 2012: pp. 422–432. <https://doi.org/10.1007/s11666-012-9871-x>
13. **Wielage, B., Grund, T., Rupprecht, C., Kümmel, S.** New Method for Producing Power Electronic Circuit Boards by Cold Gas Spraying and Investigation of Adhesion Mechanisms *Surface and Coatings Technology* 205 (4) 2010: pp. 1115–1118. <https://doi.org/10.1016/j.surfcoat.2010.06.020>
14. **Wüstefeld, C., Rafaja, D., Motylenko, M., Ullrich, C., Drehmann, R., Grund, T., Lampke, T., Wielage, B.** Local Heteroepitaxy as an Adhesion Mechanism in Aluminium Coatings Cold Gas Sprayed on AlN Substrates *Acta Materialia* 128 (1) 2017: pp. 418–427. <https://doi.org/10.1016/j.actamat.2017.02.021>
15. **Rafaja, D., Schucknecht, T., Klemm, V., Paul, A., Berek, H.** Microstructural Characterisation of Titanium Coatings Deposited Using Cold Gas Spraying on Al₂O₃ Substrates *Surface and Coatings Technology* 203 (20–21) 2009: pp. 3206–3213. <https://doi.org/10.1016/j.surfcoat.2009.03.054>
16. **Drehmann, R., Grund, T., Lampke, T., Wielage, B., Wüstefeld, C., Motylenko, M., Rafaja, D.** Essential Factors Influencing the Bonding Strength of Cold-Sprayed Aluminum Coatings on Ceramic Substrates *Journal of Thermal Spray Technology* 27 (1) 2018: pp. 446–455. <https://doi.org/10.1007/s11666-018-0688-0>
17. **Imbriglio, S.I., Nicolas, B., Maniya, A., Raynald, G., Chromik, R.R.** Influence of Substrate Characteristics on Single Ti Splat Bonding to Ceramic Substrates by Cold Spray *Journal of Thermal Spray Technology* 27 2018: pp. 1011–1024. <https://doi.org/10.1007/s11666-018-0743-x>
18. **Kümmel, S., Grund, T., Löschner, P., Wielage, B.** Influence of Deposition Conditions and Heat Treatment on Tensile Strength of Cold Spray Aluminum Coatings on Al₂O₃ and AlN Substrates. *Thermal Spray Proceedings of the International Thermal Spray Conference* 2011: pp. 1130–1135.
19. **Vidaller, M.V., List, A., Gaertner, F., Klassen, T., Dosta, S., Guilemany, J.M.** Single Impact Bonding of Cold Sprayed Ti-6Al-4V Powders on Different Substrates *Journal of Thermal Spray Technology* 24 (1) 2015: pp. 644–658. <https://doi.org/10.1007/s11666-014-0200-4>
20. **Hussain, T., McCartney, D.G., Shipway, P.H., Zhang, D.** Bonding Mechanisms in Cold Spraying: The Contributions of Metallurgical and Mechanical Components *Journal of Thermal Spray Technology* 18 (3) 2009: pp. 364–379. <https://doi.org/10.1007/s11666-009-9298-1>
21. **Kumar, S., Bae, G., Lee, C.** Influence of Substrate Roughness on Bonding Mechanism in Cold Spray *Surface and Coatings Technology* 304 (1) 2016: pp. 592–605. <https://doi.org/10.1016/j.surfcoat.2016.07.082>



© Huang et al. 2021 Open Access This article is distributed under the terms of the Creative Commons Attribution 4.0 International License (<http://creativecommons.org/licenses/by/4.0/>), which permits unrestricted use, distribution, and reproduction in any medium, provided you give appropriate credit to the original author(s) and the source, provide a link to the Creative Commons license, and indicate if changes were made.